Intermetallics 92 (2018) 72–78

Contents lists available at ScienceDirect

Intermetallics

journal homepage: www.elsevier.com/locate/intermet

Effect of the stress ratio on the fatigue behavior of $Zr_{55}Al_{10}Ni_5Cu_{30}$ bulk metallic glass part I — Analysis of the fatigue resistance

Benjamin Guennec[a,*], Takuya Nobori[b], Hirotaka Kuwahara[b], Akira Ueno[a]

[a] College of Science and Engineering, Ritsumeikan University, 1-1-1 Nojihigashi, Kusatsu, Shiga, 525-8577, Japan
[b] Graduate School of Science and Engineering, Ritsumeikan University, 1-1-1 Nojihigashi, Kusatsu, Shiga, 525-8577, Japan

ARTICLE INFO

Keywords:
Metallic glasses
Fatigue resistance and crack growth
Toughness

ABSTRACT

In the field of innovative material processing, researches dealing with the mechanical properties of Bulk Metallic Glasses (BMGs) are incontestably one of the most topical issues in the latest years. Indeed, this type of materials presents some very interesting properties, such as a high yield stress, a noticeable elongation at fracture and a good corrosion resistance. Thus, it is though that, in a near future, metallic glasses would be able to fulfill structural material applications, which are currently restricted to conventional crystalline metallic materials. However, it is already known that BMGs usually show poor fatigue properties compared to its crystalline counterparts, reducing the actual use of BMGs to non-structural applications.

Thus, such promising usages require a better understanding of the fatigue properties of BMGs, explaining the numerous works carried out to overcome this difficulty. Surprisingly, only a few literature reports are focused on the effect of the stress ratio R ($= \sigma_{min}/\sigma_{max}$) on the high-cycle fatigue behavior of BMGs. In the present work, the effect of the stress ratio, up to $R = 0.7$, on both the fatigue properties and fatigue crack propagation behavior of $Zr_{55}Al_{10}Ni_5Cu_{30}$ BMG have been studied. This first part is dealing with the fundamental fatigue resistance investigated at three distinct stress ratios of $R = 0.1$, 0.4 and 0.7. In addition, some discussions related to fracture observation will be discussed, revealing an irregularity of the fatigue crack propagation mechanism at $R = 0.7$. Finally, relative influences of both stress range and maximum stress level were analyzed using a phenomenological law.

1. Introduction

For several decades, production of metallic glasses had required very high cooling rate levels of 10^3 K s^{-1} [1], thus limiting strongly the available dimensions of samples in order to verify such a condition. However, as soon as stabilization mechanism of the supercooled liquid of some various metallic elements (Zr- [2,3], Fe- [4,5], Ti- [6,7], Pd-Cu [8] or Ni-based [9]) has been reported in the 1980's and 90's, BMGs have represented a major interest in various industry fields. Suddenly, some very interesting mechanical properties related to amorphous phase of BMGs have become available for large-scale production.

Indeed, BMGs exhibit usually high yield stresses (order of 2 GPa) and elastic strain limits (approximately 2%), inducing a potential use for structural applications [10–12]. However, BMGs also revealed particularly low fatigue endurances compared to its strengths [13–16], usually between 10% or 20% of the tensile strength. Such poor fatigue resistances were mainly attributed to the lack of microstructure that removes the possibility of a local arrest for crack propagation [13,14]. Thus a lot of researches have been conducted in order to reach higher fatigue properties of BMGs by giving a better resistance against crack propagation, or in other words by increasing its fracture toughness K_{Ic}. The very first BMG exhibiting high crack growth toughness is $Pd_{79}Ag_{3.5}P_6Si_{9.5}Ge_2$ [17], followed by the Zr-based $Zr_{61}Ti_2Cu_{25}Al_{12}$ BMG [18,19]. Interestingly, the correlation between fatigue resistance and the fracture toughness of BMGs remains not fully understood, since $Zr_{60}Cu_{30}Al_{10}$ (K_{Ic} = 110 MPa $m^{1/2}$) has been reported to be more sensitive to fatigue failure than a less tough $Zr_{50}Cu_{40}Al_{10}$ (K_{Ic} = 51 MPa $m^{1/2}$) [20]. Besides, unlike conventional crystalline metals, the fracture toughness of BMGs depends strongly on the loading rate [13,15] and the content of oxygen [21], inducing an experimental difficulty to assess the actual toughness value of the specimen under fatigue loading.

In order to get an overview of the fatigue properties of BMGs, numerous studies have been performed to better grasp the effect of several parameters on the fatigue properties and crack propagation behavior, such as effect of loading mode [22], effect of loading rate [23,24], size effect [25], effect of the environment [26–29] or effect of free volume and residual stress [15]. In the first part of the present study, the effect

* Corresponding author.
E-mail address: guennec@fc.ritsumei.ac.jp (B. Guennec).

http://dx.doi.org/10.1016/j.intermet.2017.09.023
Received 5 June 2017; Received in revised form 5 August 2017; Accepted 30 September 2017
Available online 06 October 2017

Table 1
Mechanical properties of $Zr_{55}Al_{10}Ni_5Cu_{30}$ bulk metallic glass [21,30,31].

Mechanical property	Value
Tensile strength, σ_B (MPa)	1840
Elongation (%)	2.0
Young's Modulus, E (GPa)	101
Poisson's ratio, ν	0.38
Shear modulus, G (GPa)	36.6
Bulk modulus, B (GPa)	140
Glass transition temperature T_g (K)	680
Fracture toughness K_{Ic} (MPa.m$^{1/2}$)	66.7

of stress ratio R ($= \sigma_{min}/\sigma_{max}$) on the fatigue resistance in high cycle fatigue domain of $Zr_{55}Al_{10}Ni_5Cu_{30}$ BMG has been investigated in various viewpoints. Material's *S-N* characteristics at three distinct stress ratios and general fracture surface features were studied. Furthermore, the time-dependence characteristic encountered during fatigue experiments of $Zr_{55}Al_{10}Ni_5Cu_{30}$ BMG is assessed by a phenomenological law.

2. Experimental procedures

2.1. Raw material and fatigue testing conditions

Specimens are extracted from a 10.5 mm diameter and 50 mm length round bar of $Zr_{55}Al_{10}Ni_5Cu_{30}$ BMG in atomic percentage prepared by arc melting inclination casting process. The mechanical properties of this material are indicated in Table 1 [21,30,31]. The fracture toughness K_{Ic} has been measured using Single-Edge-Pre-cracked-Bean (SEPB) method, in accordance with the ISO 15732 Standard.

For every fatigue test conducted in this work, four-point bending loading configuration is accepted. Specimen configuration consists of a rectangular beam with the following dimensions: $b = 4 \times d = 3 \times L = 40$ mm^3, where b, d and L are the specimen's width, thickness and length, respectively. In accordance with ISO 22214 Standard, the outer span is $S_1 = 30$ mm and inner span is $S_2 = 10$ mm. Direct environment of the specimen is represented in Fig. 1, where pure bending condition is verified between the two pins on the upper side of the specimen. Considering an applied load of P, one can compute the maximum bending stress σ_b exerted on the beam given by Eq. (1):

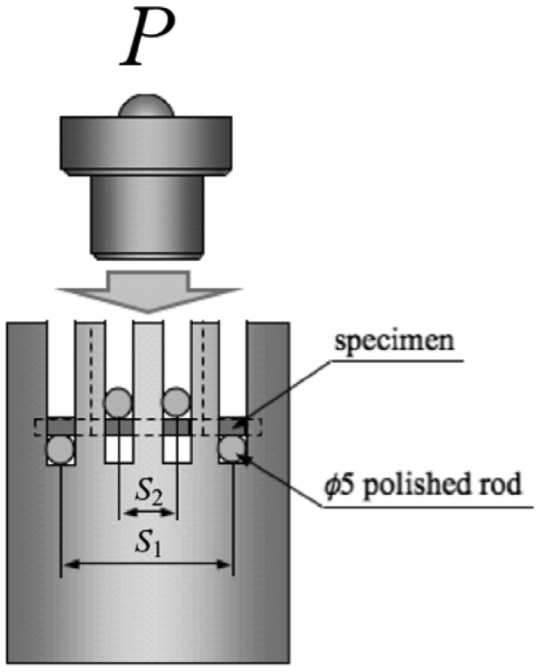

Fig. 1. Illustration of 4-point bending fatigue test's configuration.

$$\sigma_b = \frac{3P(S_1 - S_2)}{2bd^2} \quad (1)$$

Fatigue tests are carried out by a servo-hydraulic machine, under load control condition, in air and at room temperature environment. Cyclic stress obeys to a sine wave signal, with a loading frequency of 20 Hz. In the present study, three different stress ratios $R = 0.1$, 0.4 and 0.7 are accepted. The tests were terminated if specimen did not fail after 10^7 loading cycles (approximately 6 days), as commonly approved for investigation in high-cycle fatigue domain.

The specimen preparation is summarized in Fig. 2. Initially, three distinct specimens in the cross section of the raw round bar of $Zr_{55}Al_{10}Ni_5Cu_{30}$ BMG material are machined, taking attention to apply the tensile load during fatigue tests on the surfaces initially closer to the center of round bar. Then, small chamfers at 45° are introduced in order to relieve stress concentration at beam edges. The side surfaces are finished up to #4000 gridding paper, whereas the tensile surface was finally polished using 0.1-μm alumina suspension solution.

2.2. Observation of specimens after fatigue tests

In this study, observations of broken specimens were undertaken using Hitachi SU6600 SEM at a 20 kV acceleration voltage setting.

2.3. Calculation of stress intensity factor K

Fatigue crack initiation site was located at the edge (chamfer) or at the tensile surface on the specimen beam. Thus, one can assume the stress intensity factor K using the Newman-Raju formula [32] denoted in Eq. (2), assuming the quarter elliptical fracture or semi-elliptical configurations in accordance with the crack propagation configuration:

$$K = H_c \sigma_b \sqrt{\pi \frac{a}{Q}} F_c\left(\frac{a}{c}, \frac{a}{d}, \frac{c}{b}, \varphi\right), \quad (2)$$

where Hc is the bending multiplier, σb is the bending stress, Q is the configuration factor of ellipse, Φ is the angular parameter of ellipse, a and c are the depth and length of the fatigue crack, respectively. In the rest of the present paper, maximum and minimum stress intensity factor within a stress cycle are denoted Kmax and Kmin, respectively. Stress intensity factor range is $\Delta K = K\text{max} - K\text{min}$

3. Experimental results

3.1. Fundamental S-N characteristics

The most fundamental fatigue test results are presented in Fig. 3 in the form of an *S-N* curves for each stress ratio studied here ($R = 0.1$, 0.4 and 0.7), where the stress amplitude σ_a is represented in the Y-axis. The bilinear models in this diagram have been determined using the JSMS standard JSMS-SD-11-07 for *S-N* curves [33]. According to general feature of this diagram, effect of the stress ratio on the fatigue strength of $Zr_{55}Al_{10}Ni_5Cu_{30}$ BMG depends strongly on the life region considered.

On the one hand, the effect of the stress ratio is distinct in the limited fatigue life region, i.e. up to $N_f \approx 4 \times 10^4$ cycles according to Fig. 3. Indeed, in this region, one can see that the higher the stress ratio is, the lower the fatigue strength becomes. This decrease of fatigue strength is particularly obvious at the highest stress ratio $R = 0.7$. In addition, one can also notice a larger scatter of *S-N* data at $R = 0.7$ compared to the two other lower stress ratios. Furthermore, since fatigue failure occurs before 10^5 cycles regardless the stress ratio R, it is reasonable to consider $N = 10^7$ cycles as a fatigue limit in high-cycle regime.

On the other hand, the fatigue limits at 10^7 cycles σ_w found are 284 MPa, 294 MPa and 257 MPa for $R = 0.1$, 0.4 and 0.7, respectively.